Calories from carbohydrates: energetic contribution of the carbohydrate moiety of rebeccamycin to DNA binding and the effect of its orientation on topoisomerase I inhibition

Christian Bailly[1], Xiaogang Qu[2], David E Graves[3], Michelle Prudhomme[4] and Jonathan B Chaires[2]

Background: Only a few antitumor drugs inhibit the DNA breakage–reunion reaction catalyzed by topoisomerase. One is the camptothecin derivative topotecan that has recently been used clinically. Others are the glycosylated antibiotic rebeccamycin and its synthetic analog NB–506, which is presently in phase I of clinical trials. Unlike the camptothecins, rebeccamycin-type compounds bind to DNA. We set out to elucidate the molecular basis of their interaction with duplex DNA, with particular emphasis on the role of the carbohydrate residue.

Results: We compared the DNA-binding and topoisomerase-I-inhibition activities of two isomers of rebeccamycin that contain a galactose residue attached to the indolocarbazole chromophore via an α (axial) or a β (equatorial) glycosidic linkage. The modification of the stereochemistry of the chromophore–sugar linkage results in a marked change of the DNA-binding and topoisomerase I poisoning activities. The inverted configuration at the C-1′ of the carbohydrate residue abolishes intercalative binding of the drug to DNA thereby drastically reducing the binding affinity. Consequently, the α isomer has lost the capacity to induce topoisomerase-I-mediated cleavage of DNA. Comparison with the aglycone allowed us to determine the energetic contribution of the sugar residue.

Conclusions: The optimal interaction of rebeccamycin analogs with DNA is controlled to a large extent by the stereochemistry of the sugar residue. The results clarify the role of carbohydrates in stereospecific drug–DNA interactions and provide valuable information for the rational design of new rebeccamycin-type antitumor agents.

Addresses: [1]Centre Oscar Lambret et INSERM U-524, Lille 59045, France. [2]Department of Biochemistry, University of Mississippi Medical Center, Jackson, MI 39216, USA. [3]Department of Chemistry, University of Mississippi, University, MI 38677, USA. [4]UMR 6504 CNRS, Université Blaise Pascal, 63177 Aubière, France.

Correspondence: Christian Bailly and Jonathan B Chaires
E-mail: Jchaires@biochem.umsmed.edu
bailly@lille.inserm.fr

Key words: carbohydrate–DNA recognition, indolocarbazole, rebeccamycin, stereospecificity, topoisomerase I

Received: **15 January 1999**
Accepted: **9 February 1999**

Published: **7 April 1999**

Chemistry & Biology May 1999, **6**:277–286
http://biomednet.com/elecref/1074552100600277

 ISSN 1074-5521

Introduction

The indolocarbazole family is an important class of glycosylated antitumor antibiotics. This family can be divided into two subgroups depending on the nature of the linkage between the carbohydrate residue and the heterocyclic chromophore. Compounds with the sugar attached to the two indole nitrogens have little or no interaction with nucleic acids but strongly inhibit different protein kinases. This so called 'closed' form is typified by the microbial antibiotics staurosporine and K-252a that contain a pyranosyl and a furanosyl moiety, respectively (Figure 1a). They both represent very potent inhibitors of protein kinase C (PKC) and have marked cytotoxic activities [1]. This subgroup also includes the synthetic derivative UCN-01 (7-hydroxystaurosporine), which is a promising antitumor agent presently in phase I of clinical trials [2,3]. A vast number of synthetic staurosporine analogs have been synthesized with the aim of developing inhibitors that are specific for one particular PKC isoenzyme [4].

The second subgroup consists of indolocarbazole derivatives in which the carbohydrate moiety is attached to only one indole nitrogen, such as the antibiotics rebeccamycin and AT-2433-A1/B1 [5–7]. In contrast to staurosporine, rebeccamycin does not inhibit PKC in a cell-free system but interacts with DNA. The antitumor activity of rebeccamycin is attributed to its capacity to induce topoisomerase-I-dependent DNA-strand breaks [6]. Various glycosyl-substituted indolocarbazoles with an open structure like rebeccamycin specifically inhibit the DNA supercoiling enzyme topoisomerase I in a manner similar to that of the antitumor drug camptothecin [8–10]. The synthetic derivatives ED-110 and NB-506 shown in Figure 1b stabilize topoisomerase-I–DNA covalent complexes and are very potent antitumor drugs [11–13]. Recently, a phase I clinical trial with NB-506 has been successfully completed [14,15]. There is good reason to believe that this drug or a closely related congener will soon take its place as an anticancer agent.

Figure 1

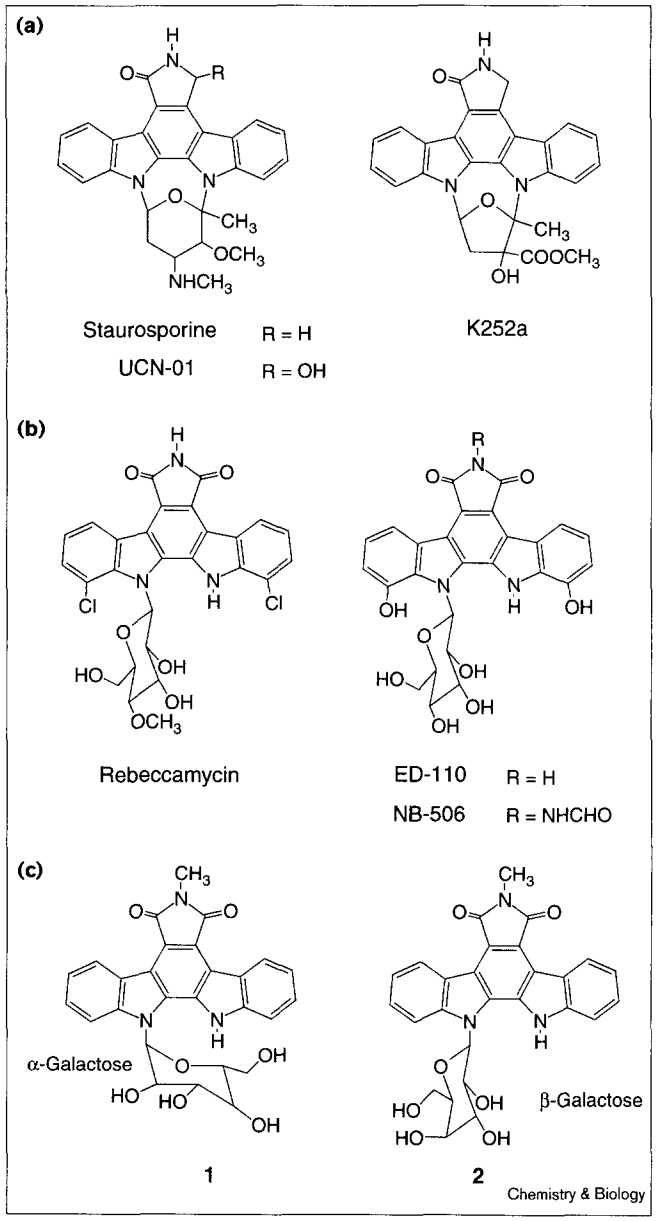

Structure of naturally occurring and synthetic antitumor indolocarbazoles. In **(a)** the drugs have a 'closed' structure with the sugar attached to the two indole nitrogens. In **(b)** the carbohydrate is attached to only one indole nitrogen and referred to as the 'open' structure. **(c)** The structure of the α and β anomers of rebeccamycin used in this study.

For both the closed and the open forms of indolocarbazoles, it is believed that the sugar unit is an important contributor to the interaction of the drug with the molecular target. In the open structures, studies have clearly shown that the removal of the sugar moiety drastically reduces the capacity of the drug to interfere with topoisomerase I [9]. More recently, we have provided direct evidence that the carbohydrate residue is a key element for both DNA binding and topoisomerase I inhibition [10].

Figure 2

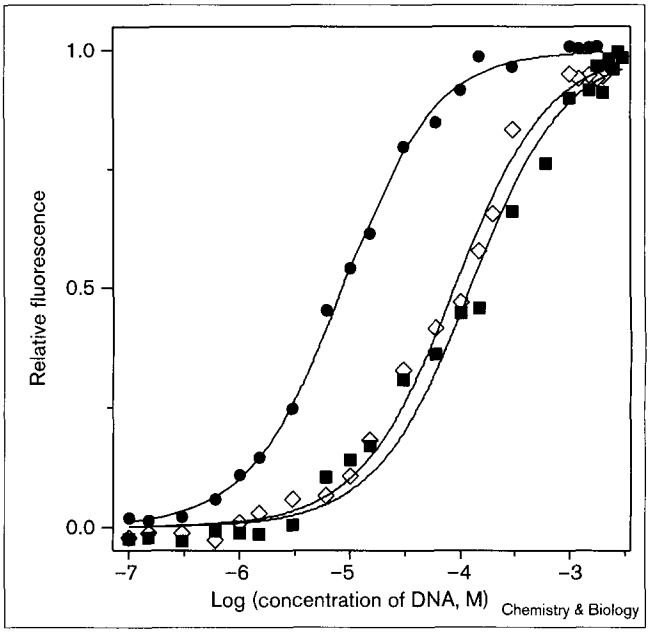

Fluorescence titrations for the interaction of the α anomer (diamonds), the β anomer (circles) and the aglycone (squares) with calf thymus DNA. The concentration of ligand was kept constant at 5 μM and the DNA concentration varied between 1 mM and 0.1 μM base pairs. The relative fluorescence, $\theta = F-F_0/F_b-F_0$, is shown as a function of DNA concentration. Curve fitting and determination of binding constants (summarized in Table 1) were carried out using nonlinear least-squares analysis.

The exact contribution of the sugar to the DNA interaction, however, is still largely unknown and is the issue we addressed here.

The present study is devoted to the characterization of the mode of binding, the affinity and the sequence selectivity of two isomeric analogs of rebeccamycin that have a galactopyranosyl residue linked to the *N*-methylindolocarbazole aglycone by either an α or a β-*N*-glycosidic bond (compounds **1** and **2**; Figure 1c). The corresponding aglycone lacking the carbohydrate domain was also tested to delinate further the contribution of the sugar residue.

Results

DNA-binding constants

Indolocarbazole derivatives are weakly fluorescent in aqueous solution but in the presence of DNA their fluorescence emission increases considerably, providing a useful means for accurately determining their DNA-binding affinities. Fluorescence-titration experiments using the aglycone and the α and β anomers are presented in Figure 2. The titration midpoints of the curves clearly differ for each drug, indicating that their binding affinities vary significantly. Nonlinear least-squares analysis of

Table 1

Binding constants and energetics of drug binding to DNA.

	F_b/F_0	$K/10^4$ (M^{-1})	$-\Delta G_{obs}$ (kcal/mol)	$-\delta \log K/\delta \log[Na^+]$	$-\Delta G_{pe}$ (kcal/mol)	$-\Delta G_t$ (kcal/mol)
α Isomer	9.5	1.14	5.42	0.30	0.72	4.70
β Isomer	107	12.6	6.81	0.33	0.79	6.02
Aglycone	5.6	0.82	5.22	0.29	0.69	4.53

Binding constant (K) and standard free energy changes (ΔG_{obs}) refer to solution conditions of 6 mM Na_2HPO_4, 2 mM NaH_2PO_4 and 1 mM Na_2EDTA, pH 7.0 at 20°C. The uncertainties in the primary experimental values K were estimated to be 10%. The polyelectrolyte contribution to the standard free energy change was calculated from the relationship $\Delta G_{pe} = (SK)\ RT\ \ln [NaCl]$, where $SK = \delta \log K/\delta \log[Na^+]$. The thermodynamic free-energy change was calculated by difference, $\Delta G_t = \Delta G_{obs} - \Delta G_{pe}$.

these titration curves yielded binding constants of 1.14×10^4 $(M\ bp)^{-1}$ and 12.6×10^4 $(M\ bp)^{-1}$ for the α and β analogs, respectively. The affinity constant of the β drug is 11-fold higher than that of its α counterpart, a difference that represents a significant stereospecificity. The binding constant measured for the α anomer is not much different from that of the aglycone (Table 1), which suggests that in the equatorial configuration the carbohydrate residue has little or no effect on the interaction with DNA. Note that the binding constant determined for the β analog by fluorescence titration is in good agreement with that determined for a related β derivative (with an OH group on the nitrogen imide instead of a CH_3 group) by absorption measurements and Scatchard analysis ($K = 17.5 \times 10^4\ M^{-1}$) [16].

The analysis of the binding constants as a function of the salt concentration confirms that the affinity of the β analog is more than one order of magnitude higher than that of the α anomer or the aglycone. Double logarithmic plots of log K versus the log of the Na^+ concentration [17] yield slopes of approximately –0.3 ($SK = \delta \log K/\delta \log [Na^+]$, Table 1), close to the theoretical value of –0.24 that is predicted for the binding of an uncharged intercalator to DNA [18]. This small slope arises from the lengthening of the DNA helix caused by intercalation, and the concomitant alteration of the charge density of the lattice, as discussed previously with another uncharged intercalating drug, hydroxyrubicin [19].

Free energy of drug binding to DNA

The observed free energy of drug binding (ΔG_{obs}) was calculated from the binding constants using the standard relationship:

$$\Delta G_{obs} = -RT \ln K \quad (1)$$

The observed binding free energy can be partitioned into the nonelectrostatic contribution (ΔG_t) and the polyelectrolyte contribution (ΔG_{pe}) by the relationship $\Delta G_{obs} = \Delta G_t + \Delta G_{pe}$. The polyelectrolyte contribution to ΔG_{obs} at a given NaCl concentration is given by the relationship [20,21]:

$$\Delta G_{pe} = (SK)\ RT \ln [Na^+] \quad (2)$$

The energetic parameters are collected in Table 1. For ΔG_{pe}, values of about –0.75 (± 0.05) kcal/mol at $[Na^+] = 16$ mM were determined for all three drugs, indicating that they bind to DNA with a slight favorable electrostatic contribution. The nonpolyelectrolyte portion is the larger contribution, however, indicating that the drug–DNA complexes are stabilized primarily by molecular interactions such as hydrogen bonding and van der Waals interactions.

Molecular modeling

Computational analysis was performed on the comparative complexation energies of the α and β isomers with two B-form DNA hexanucleotides $d(CGCGCG)_2$ and d(CGTGCG)•(CGCACG). Both DNA fragments contain CG and/or TG steps that provide appropriate drug-binding sites (see the footprinting data below). The β anomer was found to form a very stable and stereochemically feasible intercalation complex with both hexanucleotides. In contrast, attempts to build an intercalation complex with the α anomer resulted in a highly distorted DNA duplex. The chromophore of the intercalated β compound remains planar, whereas one of the rings of the intercalated α compound is out of the plane of the rest of the rings due to the steric properties of the sugar molecule. The energy-minimized intercalation model with the β isomer is shown in Figure 3.

DNA-binding mode

Previous biochemical and spectroscopic studies with different series of rebeccamycin analogs indicated that the planar indolocarbazole chromophore can intercalate into DNA [10]. Evidence that intercalation does occur for the β isomer comes from the fluorescence energy-transfer experiments shown in Figure 4. Contact energy transfer measures the energy transferred from the DNA bases to excite an intercalated fluorophore. No such energy transfer is possible for a groove- or surface-bound fluorophore because both the transfer distance and the orientation of the donor–acceptor dipoles are unfavorable [22,23]. The method has been used to provide evidence for or against

Figure 3

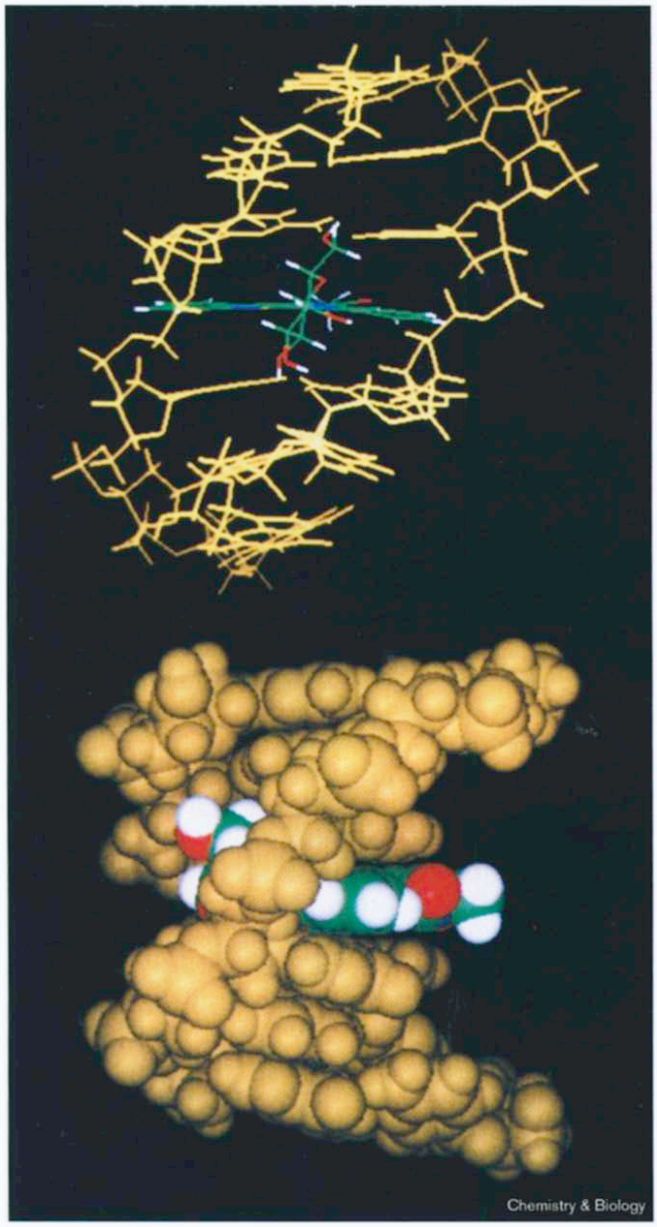

The view from the minor groove of an energy-minimized model of the complex between the β anomer and the hexanucleotide d(CGCGCG)$_2$. The molecular model illustrates the intercalation of the planar indolocarbazole chromophore and the location of the carbohydrate in the minor groove of the double helix. The structures included water and counterions (Na^+) and have been minimized to completion (root mean square < 0.001).

Figure 4

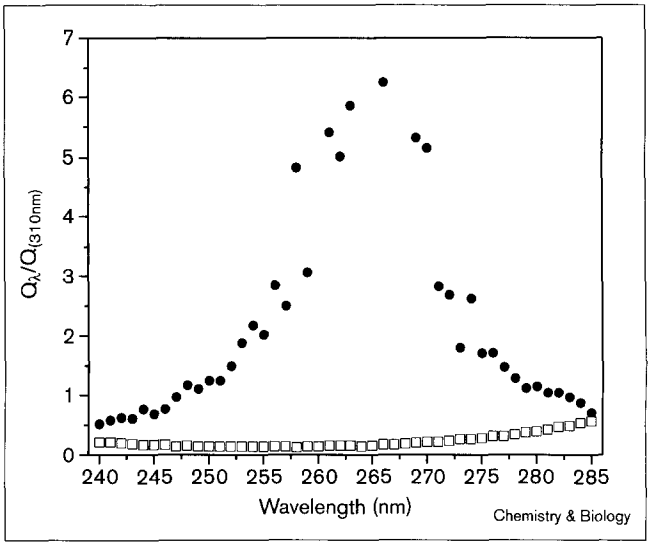

Fluorescence energy transfer from DNA to the bound drug. The relative fluorescence quantum yield of bound versus free ligand is shown as a function of excitation wavelength for the α (squares) and β (circles) anomers. See equation 5 in the Materials and methods section.

intercalation for a variety of DNA ligands, including ruthenium complexes and ethidium bromide [22,24]. As shown in Figure 4, the β derivative is excited by absorbance by DNA bases, providing evidence for intercalation. No such energy transfer occured with the α analog, suggesting that it fails to intercalate into DNA. Electric linear dichroism measurements of the drug–DNA complexes revealed identical trends. A negative reduced dichroism comparable with that measured for DNA alone at 260 nm (ΔA/A = –0.47), was measured with the β compound–DNA complex at 320 nm, whereas the reduced dichroism was considerably reduced in the presence of the α analog (ΔA/A = –0.12 and –0.48 for the α and β anomers, respectively).

We examined the emission lifetimes of the drug–DNA complexes at a single mixing ratio of 0.02 mol drug/mol bp. The fluorescence decay profiles of the drugs were bi-exponential in the presence of calf thymus DNA or with the free drug in aqueous buffer (suggesting that there are two distinct emitting species), whereas in dimethyl sulfoxide (DMSO) the decay profiles are mono-exponential. This might be a characteristic of the existence of drug–drug interactions (stacking interactions have been shown with related compounds) [25]. The extrapolated fluorescence lifetimes of the short-lived and long-lived components are listed in Table 2 together with their respective intensities. The different behaviors of DNA-bound α isomer and β isomer are quite obvious. The results are consistent with the steady-state data. The substantial lengthening of the fluorescence lifetimes for the β isomer in the presence of DNA is consistent with an intercalative binding of the indolocarbazole fluorophore.

Reactivity with chemical probes

Intercalation of a drug into DNA requires the double helix to extend and unwind to accommodate the ligand molecules between the base pairs, whereas groove binding or

Table 2

Fluorescence emission lifetimes of the drugs in the absence and presence of DNA.

	τ_1 (ns)	τ_2 (ns)	f_1	f_2	τ_a (ns)
Aglycone					
DMSO	17.7				
Buffer	4.94	0.32	0.89	0.11	4.43
+DNA	4.46	2.23	0.49	0.51	3.33
α Isomer					
DMSO	15.2				
Buffer	3.48	0.44	0.76	0.24	2.76
+DNA	3.97	0.96	0.86	0.14	3.56
β Isomer					
DMSO	16.3				
Buffer	5.00	0.54	0.55	0.45	3.00
+DNA	6.83	1.11	0.93	0.07	6.40

Average fluorescence lifetime, $\tau_a = [(f_1 \times \tau_1) + (f_2 \times \tau_2)]/(f_1 + f_2)$.

external stacking induces much less (if any) change in the DNA structure. If the β drug effectively intercalates into DNA it would be predicted to measurably distort the DNA structure, whereas the α isomer should have little effect. One way of detecting the drug-induced structural changes is through the sensitivity of the DNA to chemical probes. Accordingly, we have examined the reactivity of a ^{32}P-labeled DNA fragment towards two complementary probes, diethylpyrocarbonate and potassium permanganate, that react with purine (A>G) and pyrimidine (T>>C) residues, respectively [26]. The DNA hardly reacts at all with $KMnO_4$ in the absence of the drug, whereas in the presence of the β isomer, numerous thymine residues are rendered hyper-reactive to the probe. The $KMnO_4$ hyper-reactive thymidines are dispersed all over the entire DNA fragment, both proximal and distal to the preferred binding sites identified by footprinting (see below). This suggests that the drug-induced structural changes are distributed over several nucleotide residues around the intercalation site; such an effect has been reported for many intercalating drugs. By contrast, there is no ligand-induced hypersensitivity of the DNA towards $KMnO_4$ in the presence of the α isomer. Similar results were obtained using diethylpyrocarbonate (data not shown). The data indicate that the α and β anomers exert different effects on DNA structure, which reinforces the conclusion that the nature of the glycosidic bond is crucial for the interaction with DNA. It is conceivable that the specific effect of the α anomer on DNA structure contributes to the mechanism by which the drug inhibits topoisomerase I.

Sequence-selective binding

Footprinting experiments were performed to investigate the nucleotide sequence selectivity of the drugs. Figure 5 shows an autoradiogram resulting from the DNase I cleavage of a 3′-end-labeled 117 base pair *Eco*RI–*Pvu*II

Figure 5

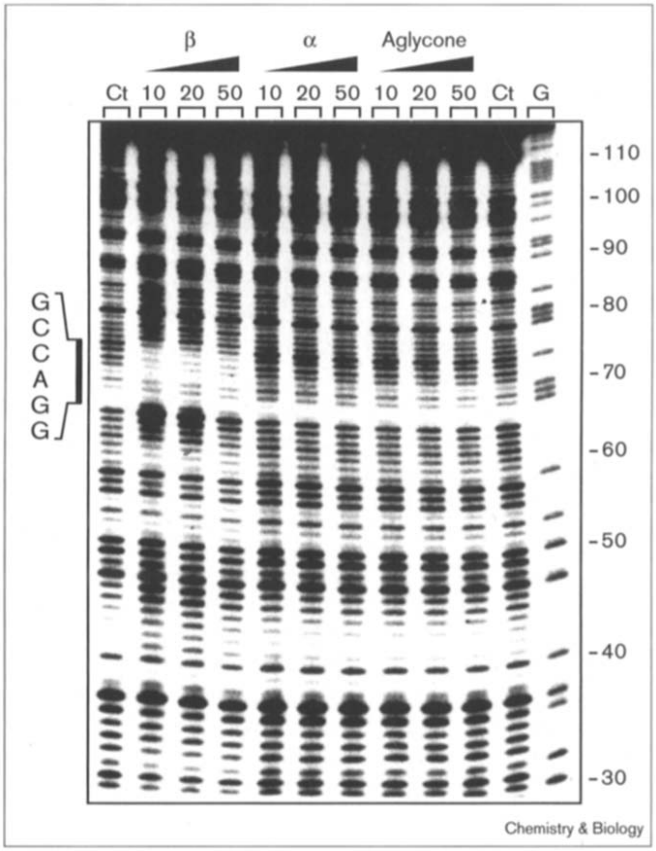

DNase I footprinting with the 117-mer *Pvu*II–*Eco*RI restriction fragment of plasmid pBS in the presence of the drugs at the indicated concentration (μM). The DNA was 3′-end labeled at the *Eco*RI site with [α-^{32}P]dATP in the presence of AMV reverse transcriptase. The products of nuclease digestion were resolved on an 8% polyacrylamide gel containing 7M urea. Control tracks (Ct) contained no drug. Guanine-specific sequence markers obtained by treatment of the DNA with dimethylsulfate followed by piperidine were run in the lane marked G. Numbers on the right side of the gel refer to the standard numbering scheme for the nucleotide sequence of the DNA fragment. The sequence of a preferential binding site for the β anomer is indicated on the left-hand side.

restriction fragment from plasmid pBS in the absence and presence of the test drugs. The β isomer alters the DNAase I cleavage profile, whereas the α isomer and the aglycone have no effect. The major sequence protected by the β isomer from cleavage by DNase I corresponds to 5′-GCCAGG between positions 68 and 73. In addition, the drug increases the susceptibility to DNase I cleavage at A•T-rich sequences (e.g. around nucleotide position 65, 5′-TTTT-3′). Additional footprinting experiments were performed with three other DNA fragments to assess the sequence selectivity of the tested compounds with respect to a wide variety of potential binding sites. In each case, we detected footprints exclusively with the β isomer, at sequences such as 5′-AGTGAGTCG-3′ and 5′-CCTCTAG-3′. There were absolutely no footprints

with the corresponding α anomer. The binding of the β compound to GC sequences is therefore favoured over binding to A•T or to mixed sequences. We have recently reported similar results using another series of rebeccamycin analogs [16].

Topoisomerase I poisoning

Two complementary biochemical assays were performed to compare the capacity of the indolocarbazole drugs to inhibit topoisomerase I. First we studied DNA relaxation. Negatively supercoiled plasmid pAT was incubated with both human topoisomerase I and the test drug at 30 μM. The DNA samples were treated with sodium dodecylsulfate (SDS) and proteinase K to remove any covalently bound protein and were then resolved in a 1% agarose gel. The gel shown in Figure 6 indicates that the β isomer inhibits the relaxation of DNA mediated by topoisomerase I, whereas both the α isomer and the aglycone have little or no effect.

The inhibition of DNA relaxation observed with the β isomer can arise from stabilization of topoisomerase I–DNA cleavable complexes or it can be a result of saturating the DNA and preventing the enzyme from binding to the plasmid. The latter nonspecific effect due to template binding is known to be important with DNA-intercalating agents. This compound can also function as a specific topoisomerase I inhibitor, however, trapping the cleavable complexes. To examine further the activity of the drug on the enzyme, the topoisomerase cleavage sites induced by the drugs were mapped using a 160 base pair DNA fragment. The *Eco*RI–*Ava*I restriction fragment from plasmid pAT was uniquely end-labeled at the 3′-end of the lower strand at the *Eco*RI site and used as a substrate for the topoisomerase-I-cleavage reaction. The cleavage products were analyzed on a sequencing polyacrylamide gel (Figure 7). It can be seen unambiguously that the β isomer (and the reference topoisomerase I inhibitor camptothecin), but not the α isomer, strongly promote DNA cleavage by human topoisomerase I. Although in several cases the cleavage occurs principally at sites that have a thymine and a guanine on the 5′ and 3′ sides of the cleaved bond, respectively (see [10] for a statistical analysis of the cleavage specificity), it is clear that cutting can sometimes occur at different nucleotide positions. These data indicate that the β-*N*-glycosydic linkage represents a key element for topoisomerase I inhibition, as well as for DNA intercalation as mentioned above.

Figure 6

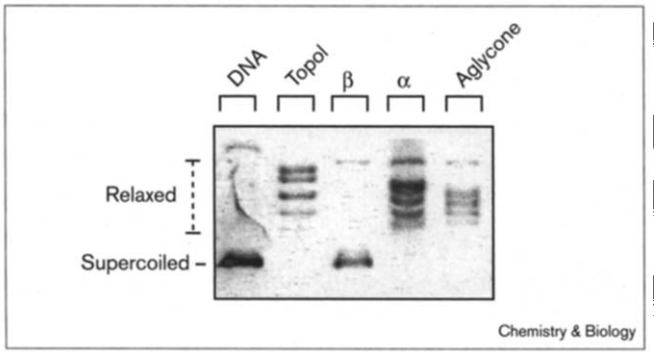

Inhibition of topoisomerase-I-mediated DNA supercoiling in the presence of the drugs. Native supercoiled pAT DNA (0.5 μg; lane DNA) was incubated for 30 min at 37°C with 2 units of topoisomerase I in the absence (lane Topol) or in the presence of test drug at 30 μM. The reaction was stopped with SDS and treatment with proteinase K. The DNA was analyzed by native agarose gel electrophoresis. The gels were stained with ethidium bromide and photographed under UV light.

Discussion

Results obtained using a multifaceted experimental approach show clear contrasting behavior between rebeccamycin analog stereoisomers. The β compound exhibits a high affinity for DNA and forms intercalation complexes. It binds selectively to GC-rich sequences in DNA and is a potent inhibitor of topoisomerase I. The α anomer, in contrast, binds more weakly to DNA than does the β compound, does not intercalate and does not inhibit topoisomerase I. We conclude that altering the stereochemistry of the sugar attachment changes the mode of binding of the anomer to DNA and the capacity of the drug to interfere with topoisomerase I.

The binding free energy contribution from the carbohydrate can be estimated from the difference in the binding free energy of the β glycoside (ΔG_β) and the aglycone ($\Delta G_{aglycone}$), $\Delta G_\beta - \Delta G_{aglycone} = -1.6$ kcal/mol. This value is close to that calculated for the difference between the β and α glycosides, $\Delta\Delta G_{\beta-\alpha} = -1.4$ kcal/mol. The lack of significant difference between the β-glycoside and the aglycone in terms of binding free energy suggests that the α sugar plays little or no part in the interaction of the drug with DNA. (We note that in computing these differences in free energy changes, we neglect possible entropic contributions to an interaction free energy term that formally must be included in the difference.) These free energy differences show clearly that the β carbohydrate makes a significant contribution to the binding free energy. The β anomer binding free energy is about 1.4–1.6 kcal/mol more favorable than that observed with the α anomer or with the aglycone, most probably because of the formation of favorable noncovalent molecular interactions between the carbohydrate and the DNA. The molecular model shown in Figure 3 is consistent with this idea. The energetics data demonstrate unambiguously that the drug–DNA interaction process is stereospecific with respect to the carbohydrate linkage.

The energetic contribution of the carbohydrate moiety of the anthracycline antibiotics [19,27] provides an interesting

Figure 7

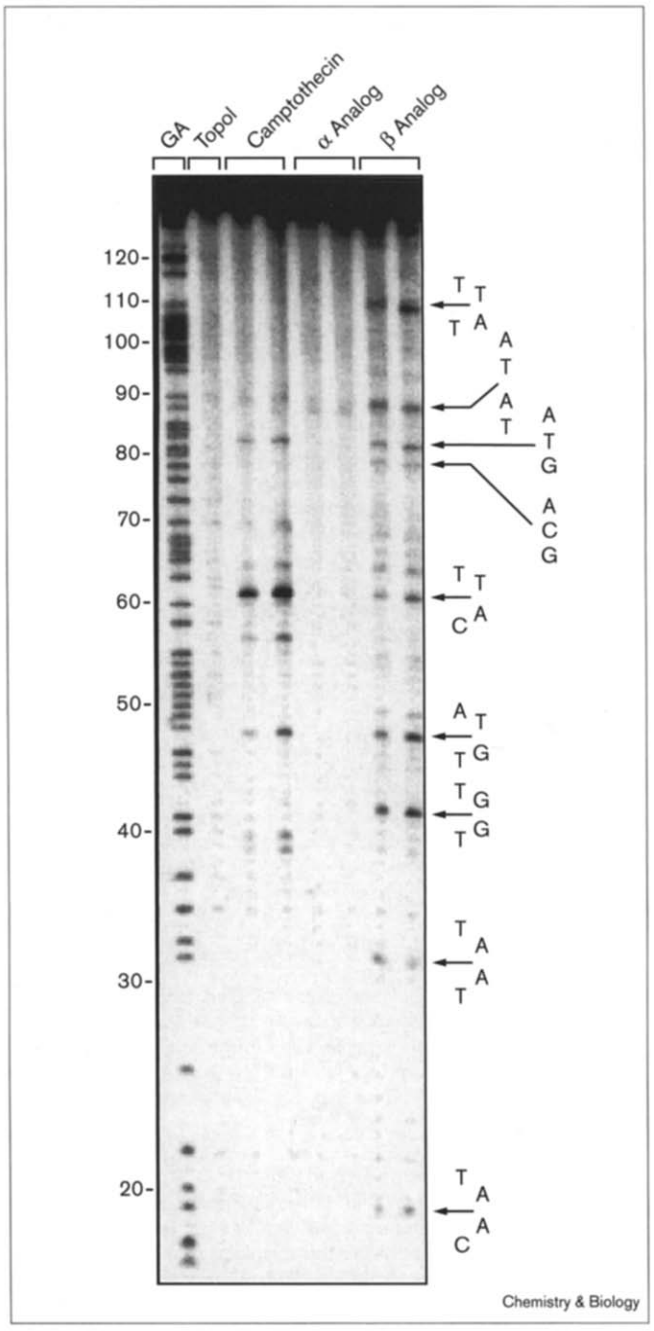

Phosphorimage comparing the susceptibility of the 160 base pair *tyr*T fragment to cutting by topoisomerase I in the presence of the two anomeric compounds. The 5′-end-labeled fragment was incubated in the absence (lane Topol) or presence of the indolocarbazole derivatives or camptothecin (25 μM each) for 45 min at 37°C. Reactions were stopped with SDS and treatment with proteinase K. Topoisomerase-I-cleavage reactions were analyzed on an 8% denaturing polyacrylamide gel as described in the Materials and methods section. Numbers to the left of the gel show the nucleotide position, determined with reference to the purine nucleotide tracks labeled G+A. The positions of the cleavage sites promoted by the β anomer are indicated by arrows with the corresponding sequences.

comparison to the data reported here. Doxorubicin, the prototype anthracycline, contains the carbohydrate daunosamine, which is positively charged at physiological pH and which can make a favorable free-energy contribution of up to –4 kcal/mol to the overall binding free energy from the polyelectrolyte (ΔG_{pe}) effect alone [28]. Under the same salt concentrations as used in the present study, ΔG_{pe} was found to be –2.6 kcal/mol for doxorubicin. In contrast, the rebeccamycin compounds studied here lack such a large polyelectrolyte contribution because they are uncharged, reflected in the modest values of ΔG_{pe} reported in Table 1. The daunosamine, however, contributes an additional favorable free-energy increment of about –2 kcal/mol, above and beyond its polyelectrolyte contribution [27]. This contribution reflects the favorable molecular interactions from fitting the daunosamine into the minor groove, resulting in van der Waals attractions and possible hydrogen-bonding interaction between the amine group and DNA bases. The magnitude of this part of the daunosamine energetic contribution is comparable to the value of $\Delta G_{\beta}-\Delta G_{aglycone} = -1.6$ kcal/mol that was estimated for rebeccamycin, which probably reflects similar favorable molecular interactions of the carbohydrate moiety in the minor groove. Finally, there is a very interesting contrast between doxorubicin and rebeccamycin stereoisomers with respect to their contributions to DNA-binding free energy. For rebeccamycin, the energetic difference between the β and α isomers is essentially the same as that observed between the β isomer and the aglycone. In contrast, the β anomer of doxorubicin bound to DNA with considerably less affinity than the aglycone, indicating a steric penalty for incorrect positioning of the carbohydrate moiety [27]. For doxorubicin binding to DNA, it is energetically more favorable to lack daunosamine than to have it in the wrong orientation. This is not the case for the stereoisomers of rebeccamycin.

The rebeccamycin isomers described here are not the only anticancer agents that require a glycosyl residue for their mechanism of action. Many antitumor drugs contain a saccharide domain that contributes significantly to their interactions with DNA [29,30]. One well-known case is that of the enediyne family of DNA-cleaving antitumor antibiotics. The aryltetrasaccharide moiety of calicheamycin γ_1I, for example, plays a critical role in the sequence-selective recognition of tetranucleotide sequences such as TCCT, TCTC or TTTT, in addition to contributing positively to the DNA-cleavage activity of the antibiotic [31–35]. The carbohydrate portion of calicheamycin not only reads the minor-groove sequence but most importantly it orients the reactive enediyne aglycone, placing the proradical center adjacent to the cleavage site. A similar warhead alignment mediated by the oligosaccharide moiety occurs with the related drug esperamicin A_1 [36]. Moreover, the glycosyl domain of calicheamycin is essential

for the inhibition of transcription by polymerase II, probably by inducing a conformational change in DNA structure [37,38]. With neocarzinostatin, another diyene antibiotic, the aminoglycoside residue is not a major determinant of base specificity of DNA cleavage but plays a major functional role in improving the rate and efficiency of DNA cleavage [39]. Many other drugs including the bleomycins, the pluramycins and the aureolic acids (e.g. mithramycin, chromomycin and olivomycin) possess DNA-interacting carbohydrate domains. With the aminoglycoside antibiotics such as tobramycin and neomycin, molecular recognition of a defined RNA conformation depends entirely on the structure of the saccharide [40]. With daunomycin, high-resolution nuclear magnetic resonance (NMR) and crystal structural studies show that the sugar residue participates in specific hydrogen-bonding interactions with DNA bases, along with numerous van der Waals interactions with atoms in the minor groove [41–43].

The pronounced differences between the DNA-binding and toposisomerase-I-inhibition activities of the α and β isomers of the indolocarbazole analogs described here represent another example of the key role played by carbohydrates in the molecular recognition of DNA.

Significance

Rebeccamycin and its indolocarbazole analogs are promising antitumor agents, and two synthetic derivatives NB-506 and ED-749 are currently in clinical trials for potential use in cancer chemotherapy. The cytotoxicity of these molecules depends on their capacity to interact with DNA and to inhibit topoisomerase I. The rational design of rebeccamycin analogs requires, therefore, a precise understanding of the molecular rules governing the recognition of DNA and/or DNA–topoisomerase I complexes by the drugs. Our present study has clarified the role of the carbohydrate portion of the drug in its interaction with the DNA double helix. The β→α inversion of the configuration of the sugar–indolocarbazole linkage considerably reduces the affinity of the drug for DNA, and impedes its capacity to form intercalation complexes and to inhibit topoisomerase I. The results reveal that the interaction of rebeccamycin analogs with DNA is controlled to a large extent by the sugar residue and that the isomery of the glycosidic linkage is essential. The drug–DNA interaction process is stereospecific. As such, the results expand our knowledge of drug–DNA interactions and provide invaluable information for the design of rebeccamycin-type antitumor agents.

Materials and methods

Drugs

The synthesis of the drugs has been reported previously [44]. Stock solutions of the α and β isomers were freshly prepared at a concentration of 2 mM in DMSO, and diluted into buffer solution at the desired concentration.

Instrumentation

Absorbance spectra were recorded on a Cary 3E UV/Vis spectrophotometer equipped with a thermoelectric temperature controller. Fluorescence measurements were done with an ISS Inc. Greg 200 fluorometer, operated in a steady-state, photon-counting mode. Fluorescence lifetimes were measured using an ISS Inc. K2 multi-frequency phase fluorometer.

Determination of binding constants by fluorescence titration experiments

Stock solutions of compounds were freshly prepared at a concentration of 2 mM in DMSO, and diluted into buffer solution at the desired concentration. Calf thymus DNA was purchased from Pharmacia (Lot No. 27-4562-02) and was sonicated and purified as described previously [19]. Before further use, the DNA was dialyzed in the appropriate buffer for 24 h, and its concentration was determined by UV absorption at 260 nm using a molar extinction coefficient, $\varepsilon_{260} = 12{,}824\ cm^{-1}M^{-1}$. Titration experiments were carried out in a buffer consisting of 6 mM Na_2HPO_4, 2 mM NaH_2PO_4, 1 mM Na_2EDTA, pH 7.0, unless noted otherwise. Fluorescence titration data were recorded at room temperature, with excitation at 320 nm and fluorescence emission was monitored over the range of 340–620 nm. For titration experiments, each sample was prepared separately at a constant drug concentration of 5 μM, and DNA concentrations ranging from 0.1 μM to 1 mM base pair.

Fluorescence titration data were fit directly to get binding constants, using a fitting function incorporated into the program FitAll (MTR Software, Toronto). The observed fluorescence is assumed to be a sum of the weighted concentrations of free and bound ligand:

$$F = F^0 (C_t - C_b) + F^b C_b \quad (3)$$

where F is the apparent fluorescence at each DNA concentration, F^0 is the fluorescence intensity of free ligand, and F^b is the fluorescence intensity of the bound species. C_t and C_b are the molar concentrations or total and bound ligand, respectively. For the interaction of a ligand D with a DNA site S, it can be easily shown that:

$$Kx^2 - x(KS_0 + KD_0 + 1) + KS_0D_0 = 0 \quad (4)$$

Where $x = C_b$, K is the association constant, S_0 is the total site concentration and D_0 is the total ligand concentration. Equation 4 is readily solved using the quadratic formula. Data in the form of fluorescence response F as a function of total DNA site concentration at fixed concentration of ligand may then be fit by nonlinear least-squares methods to get K, F^0 and F^b.

Fluorescence contact energy transfer

Contact energy transfer from DNA bases to ligand was measured from corrected excitation spectra recorded from 240 nm to 350 nm at 1 nm intervals [24]. The ratio between the quantum yield of bound ligand with excitation in the UV spectral region (Q_λ) to that at 310 nm (Q_{310}) was calculated from the expression:

$$\frac{Q_\lambda}{Q_{310}} = \left[\frac{I_\lambda E_{310}}{I_{310} E_\lambda}\right]_b \left[\frac{I_{310} E_\lambda}{I_\lambda E_{310}}\right]_f \quad (5)$$

where I and E are the measured fluorescence intensities and molar extinction coefficient, respectively. The subscripts *b* and *f* refer to the bound and free forms of the ligand. The wavelength 310 nm was chosen for normalization because of the negligible absorbance of DNA in that region of the spectrum. Excitation spectra were corrected for inner filter effects prior to normalization.

Molecular-modeling studies

Molecular modeling using the programs Discover and INSIGHT II (Molecular Simulations, Inc.) were performed on the α, β and aglycone analogs of rebeccamycin. Drug structures were constructed using the

BUILDER program of INSIGHT II. Charge distribution and energy minimized structures were obtained using the program MOPAC (MNDO) and the conjugate-gradient minimization algorithm. Duplex B–DNA structures of sequences $d(CGCGCG)_2$ and d(CGTGCG)•(CGCACG) were constructed using the BIOPOLYMER program of INSIGHT II. Counterions (sodium atoms) were added at a distance of 2.5 Å from each phosphate to these duplex DNAs. Ligands were manually docked within the central 5′-CpG-3′ or 5′-TpG-3′ steps of the oligonucleotides to minimize close contacts between the ligand and DNA. Insertion of the ligand between these base pairs effectively opened the intercalation site to accommodate the DNA-binding ligand. Periodic boundary conditions were imposed on the ligand–DNA complex with an additional 3.5 Å space added to all sides of the complex. The solvation routine of INSIGHT II was then used to add water molecules to the ligand–DNA duplex structure. Atomic potentials were added to all atoms of the assembly using the AMBER forcefield. The hydrated ligand–DNA complex was then subjected to energy minimization under periodic boundary conditions using 1000 steepest-descent iterations to reduce the maximum root mean squared (rms) derivative to less than 0.5, followed by 10,000 iterations using the conjugate-gradient method to reduce the maximum rms derivative to less than 0.001. A distance-dependent dielectric constant of 1.0 was used for these calculations. Computations were performed on a Silicon Graphics Indigo Elan workstation and visualized using INSIGHT II.

DNA purification and labeling

The plasmid pBS (Stratagene, La Jolla, California) was isolated from *Escherichia coli* by a standard SDS–sodium hydroxide lysis procedure and purified using Qiagen columns. The purified plasmid was then precipitated and resuspended in appropriate buffered medium prior to digestion by the restriction enzymes. The two pBS DNA fragments were prepared by 3′-[^{32}P]-end labeling of the *Eco*RI–*Pvu*II double digest of the plasmid using α-[^{32}P]-dATP and avian myeblastosis virus (AMV) reverse transcriptase. The digestion products were separated on a 6% polyacrylamide gel under native conditions in TBE buffered solution (89 mM Tris–borate pH 8.3, 1 mM EDTA). After autoradiography, the band of DNA was excised, crushed and soaked in water overnight at 37°C. This suspension was filtered through a Millipore 0.22 μm filter and the DNA was precipitated with ethanol. Following washing with 70% ethanol and vacuum drying of the precipitate, the labeled DNA was resuspended in 10 mM Tris adjusted to pH 7.0 containing 10 mM NaCl.

Footprinting experiments

Samples (3 μl) of the ^{32}P-labeled DNA fragment were incubated with 5 μl of the buffer solution containing the desired drug concentration. After 20 min incubation at 37°C to ensure equilibration of the binding reaction, the digestion was initiated by the addition of 2 μl of DNase I (0.01 unit ml^{-1} enzyme in 20 mM NaCl, 2 mM $MgCl_2$, 2 mM $MnCl_2$, pH 7.3). At the end of the reaction time (routinely 4 min at room temperature), the digestion was stopped by freeze-drying. After lyophilization each sample was resuspended in 4 μl of an 80% formamide solution containing tracking dyes prior to electrophoresis.

Topoisomerase I inhibition

Relaxation assay. Supercoiled pKMp27 DNA (0.5 μg) was incubated with 3 units human topoisomerase I (TopoGen Inc, Columbus, Ohio) at 37°C for 1 h in relaxation buffer (50 mM Tris pH 7.8, 50 mM KCl, 10 mM $MgCl_2$, 1 mM dithiothreitol, 1 mM EDTA) in the presence of the drug under study at the indicated concentration. Reactions were terminated by addition of SDS and proteinase K. DNA samples were then added to the electrophoresis dye mixture (3 ml) and electrophoresed (35V cm^{-1}) in a 1% agarose gel at room temperature for 15 h. Gels were stained with ethidium bromide (1 mg ml^{-1}), washed and photographed under UV light.

Sequencing of topoisomerase-I-mediated DNA cleavage sites. Each reaction mixture contained 2 μl of 3′-end [^{32}P] labeled DNA (~1 μM), 5 μl of water, 2 μl of 10× topoisomerase I buffer, 10 μl of drug solution at the desired concentration (50 μg ml^{-1}). After at least 30 min incubation to ensure equilibration, the reaction was initiated by addition of 10 units topoisomerase I. Samples were incubated for 40 min at 37°C prior to adding SDS to 0.25% and proteinase K to 250 μg ml^{-1} to dissociate the drug–DNA–topoisomerase-I cleavable complexes. The DNA was precipitated with ethanol and then resuspended in 5 ml formamide–TBE loading buffer, denatured at 90°C for 4 min then chilled on ice for 4 min prior to loading onto the sequencing gel.

Acknowledgements

Supported by grants from the Association pour la Recherche sur le Cancer (C.B.), the Ligue Nationale contre le Cancer (Comite du Nord) (C.B.), the National Cancer Institute (CA35635 to J.B.C.) and from the National Science Foundation (MCB-9728720 to D.G.). Thanks to Jinsong Ren for her comments on the manuscript.

References

1. Ruegg, U.T. & Burgess, G.M. (1989). Staurosporine, K-252a, and UCN-01: potent but nonspecific inhibitors of protein kinase. *Trends Pharmacol. Sci.* **10**, 218-220.
2. Akinaga, S., Gomi, K., Morimoto, M., Tamaoki, T. & Okabe, M. (1991). Antitumor activity of UCN-01, a selective inhibitor of protein kinase C, in murine and human tumor models. *Cancer Res.* **51**, 4888-4892.
3. Shao, R.G., Cao, C.X., Shimizu, T., O'Connor, P.M., Kohn, K.W. & Pommier, Y. (1997). Abrogation of an S-phase checkpoint and potentiation of camptothecin cytotoxicity by 7-hydroxystaurosporine (UCN-01) in human cancer cell lines, possibly influenced by p53 function. *Cancer Res.* **57**, 4029-4035.
4. Prudhomme, M. (1997). Indolocarbazoles as anti-cancer agents. *Curr. Pharm. Des.* **3**, 265-290.
5. Nettleton, D.E., Doyle, T.W., Krishnan, B., Matsumoto G.K. & Clardy, J. (1985). Isolation and structure of rebeccamycin – a new antitumor antibiotic from *Nocardia aerocolonigenes*. *Tetrahedron Lett.* **26**, 4011-4014.
6. Bush, J.A., Long, B.H., Catino, J.J., Bradner, W.T. & Tomita, K. (1987). Production and biological activity of rebeccamycin, a novel antitumor agent. *J. Antibiotics* **40**, 668-678.
7. Matson, J.A., *et al.* & Patel, M. (1989). AT2433-A1, AT2433-A2, AT2433-B1 and AT2433-B2, novel antitumor antibiotic compounds produced by *Actinomadura malliaura*. *J. Antibiot.* **42**, 1547-1555.
8. Yamashita, Y., Fujii, N., Murakata, C., Ashizawa, T., Okabe, M. & Nakano, H. (1992). Induction of mammalian DNA topoisomerase I mediated DNA cleavage by antitumor indolocarbazole derivatives. *Biochemistry* **31**, 12069-12075.
9. Rodrigues-Pereira E., *et al.* & Fabbro, D. (1996). Structure-activity relationships in a series of substituted indolocarbazoles: topoisomerase I and protein kinase C inhibition and antitumoral and antimicrobial properties. *J. Med. Chem.* **39**, 4471-4477.
10. Bailly, C., Riou, J.F., Colson, P., Houssier, C., Rodrigues-Pereira, E. & Prudhomme, M. (1997). DNA cleavage by topoisomerase I in the presence of indolocarbazole derivatives of rebeccamycin. *Biochemistry* **36**, 3917-3929.
11. Yoshinari, T., *et al.*, & Okura, A. (1993). Induction of topoisomerase-I-mediated DNA cleavage by a new indolocarbazole, ED-110. *Cancer Res.* **53**, 490-494.
12. Yoshinari, T., *et al.*, & Nishimura, S. (1995). Novel antitumor indolocarbazole compound 6-*N*-formylamino-12,13-dihydro-1,11-dihydroxy-13-(β-D-glucopyranosyl)-5*H*-indolo[2,3-a]pyrrolo-[3,4-c]carbazole-5,7-(6*H*)-dione (NB-506): induction of topoisomerase-I-mediated DNA cleavage and mechanisms of cell line-selective cytotoxicity. *Cancer Res.* **55**, 1310-1315.
13. Arakawa, H., *et al.*, & Nishimura, S. (1995). Novel indolocarbazole compound 6-*N*-formylamino-12,13-dihydro-1,11-dihydroxy-13-(β-D-glucopyranosyl)-5*H*-indolo[2,3-a]pyrrolo-[3,4-c]carbazole-5,7-(6*H*)-dione (NB-506): its potent antitumor activities in mice. *Cancer Res.* **55**, 1316-1320.
14. Ohe, Y., *et al.*, & Sasaki, Y. (1997). Phase I and pharmacology study of 5-day infusion of NB-506. *Proc. ACSO* **16**, 199a.
15. Saijo, N. (1998). New chemotherapeutic agents for the treatment of non-small cell lung cancer. *Chest* **113**, 17S-25S.
16. Bailly, C., Colson, P., Houssier, C., Rodrigues-Pereira, E., Prudhomme, M. & Waring, M.J. (1998). Recognition of specific sequences in DNA by a topoisomerase I inhibitor derived from the antitumor drug rebeccamycin. *Mol. Pharmacol.* **53**, 77-87.

17. Record, M.T., Anderson, C.F. & Lohman, T.M. (1978). Thermodynamic analysis of ion effects on the binding and conformational equilibria of proteins and nucleic acids: the role of ion association or release, screening, and ion effects on water activity. *Quart. Rev. Biophys.* **11**, 103-178.
18. Friedman, R.A. & Manning, G.S. (1984). Polyelectrolyte effects on site-binding equilibria with application to the intercalation of drugs into DNA. *Biopolymers* **23**, 2671-2714.
19. Chaires, J.B., Priebe, W., Graves, D.E. & Burke, T.G. (1993). Dissection of the free energy of anthracycline antibiotic binding to DNA: electrostatic contributions. *J. Am. Chem. Soc.* **115**, 5360-5364.
20. Record, M.T., Jr. & Spolar. R. (1990). Some thermodynamic principles of nonspecific and site-specific protein–DNA interactions. *The Biology of Nonspecific DNA–Protein Interactions.* (Revzin, A., ed.). pp. 33-69, CRC Press, Boca Raton, FL.
21. Record, M.T., Jr., Ha, J.H. & Fisher, M.A. (1991). Analysis of equilibrium and kinetic measurements to determine thermodynamic origins of stability and specificity and mechanism of formation of site-specific complexes between proteins and helical DNA. *Methods Enzymol.* **208**, 291-343.
22. Le Pecq, J.B. & Paoletti, C. (1967). A fluorescent complex between ethidium bromide and nucleic acids. *J. Mol. Biol.* **27**, 87-106.
23. Suh, D. & Chaires, J.B. (1995). Criteria for the mode of binding of DNA binding agents. *Bioorg. Med. Chem.* **3**, 723-728
24. Haq, I., Lincoln, P., Suh, D., Norden, B., Chowdhry, B.Z. & Chaires, J.B. (1995). Interaction of Δ- and Λ-[Ru(phen)2DPPZ]$^{2+}$ with DNA: a calorimetric and equilibrium binding study. *J. Am. Chem. Soc.* **117**, 4788-4796.
25. Moreau, P., *et al.*, & Aubertin, A.M. (1998). Syntheses and biological evaluation of indolocarbazoles, analogs of rebeccamycin, modified at the imide heterocycle. *J. Med. Chem.* **41**, 1631-1640.
26. Bailly, C. & Waring, M.J. (1997). Diethylpyrocarbonate and osmium tetroxide as probes for drug-induced changes in DNA conformation *in vitro*. In *Drug–DNA Interactions: Methods, Case Studies, and Protocols. Methods in Molecular Biology, volume 90.* (Fox, K.R., ed). pp. 51-79, Humana Press, Totowa, NJ.
27. Chaires, J.B., Satyanarayana, S., Suh, D., Fokt, I., Przewloka, T. & Priebe, W. (1996). Passing the free energy of anthracycline antibiotic binding to DNA. *Biochemistry* **35**, 2047-2053.
28. Chaires, J.B. (1996). Dissecting the free energy of drug binding to DNA. *Anti-Cancer Drug Des.* **11**, 569-580.
29. Kahne, D. (1995). Strategies for the design of minor groove binders: a re-evaluation based on the emergence of site-selective carbohydrate binders. *Chem. Biol.* **2**, 7-12.
30. Sears, P. & Wong, C.H. (1996). Intervention of carbohydrate recognition by proteins and nucleic acids. *Proc. Natl Acad. Sci. USA* **93**, 12086-12093.
31. Nicolaou, K.C., Tsay, S.C., Suzuki, T. & Joyce, G.F. (1992). DNA–carbohydrate interactions. Specific binding of the calicheamicin γ_1^I oligosaccharide with duplex DNA. *J. Am. Chem. Soc.* **114**, 7555-7557.
32. Paloma, L.G., Smith, J.A., Chazin, W.J. & Nicolaou, K.C. (1994). Interaction of calicheamicin with duplex DNA: role of the oligosaccharide domain and identification of multiple binding modes. *J. Am. Chem. Soc.* **116**, 3697-3708.
33. Ikemoto, N., Kumar, R.A., Ling, T.T., Ellestad, G.A., Danishefsky, S.J. & Patel, D.J. (1995). Calicheamicin–DNA complexes: warhead alignment and saccharide recognition of the minor groove. *Proc. Natl Acad. Sci. USA* **92**, 10506-10510.
34. Chatterjee, M., Smith, P.J. & Townsend, C.A. (1996). The role of the aminosugar and helix binding in the thiol-induced activation of calicheamicin for DNA cleavage. *J. Am. Chem. Soc.* **118**, 1938-1948.
35. Kumar, R.A., Ikemoto, N. & Patel, D.J. (1997). Solution structure of the calicheamicin γ_1^I–DNA complex. *J. Mol. Biol.* **265**, 187-201.
36. Kumar, R.A., Ikemoto, N. & Patel, D.J. (1997). Solution structure of the esperamicin A_1–DNA complex. *J. Mol. Biol.* **265**, 173-186.
37. Liu, C., *et al.*, & Vogt, P.K. (1996). Sequence-selective carbohydrate-DNA interaction: dimeric and monomeric forms of calicheamicin oligosaccharide interfere with transcription factor function. *Proc. Natl Acad. Sci. USA* **93**, 940-944.
38. Ho, S.N., Boyer, S.H., Schreiber, S.L., Danishefsky, S.J. & Crabtree, G.R. (1994). Specific inhibition of formation of transcription complexes by a calicheamicin oligosaccharide: a paradigm for the development of transcriptional antagonists. *Proc. Natl Acad. Sci. USA* **91**, 9203-9207.
39. Myers, A.G., Kort, M.E. & Hammond, M. (1997). A comparison of DNA cleavage by neocarzinostatin chromophore and its aglycone: evaluating the role of the carbohydrate residue. *J. Am. Chem. Soc.* **119**, 2965-2972.
40. Jiang, L., Suri, A.K., Fiala, R. & Patel, D.J. (1997). Saccharide–RNA recognition in an aminoglycoside antibiotic–RNA aptamer complex. *Chem. Biol.* **4**, 35-50.
41. Wang, A.H.J., Ughetto, G., Quigley, G.J. & Rich, A. (1987). Interactions between an anthracycline antibiotic and DNA: molecular structure of daunomycin complexed to d(CpGpTpApCpG) at 1.2 Å resolution. *Biochemistry* **26**, 1152-1163.
42. Frederick, C. A., *et al.*, & Wang, A. H.-J. (1990). Structural comparison of anticancer drug–DNA complexes: adriamycin and daunomycin. *Biochemistry* **29**, 2538-2549.
43. Chaires, J.B. (1990). Biophysical chemistry of the daunomycin–DNA interaction. *Biophys. Chem.* **35**, 191-202.
44. Anizon, F., *et al.*, & Meyer, T. (1997). Syntheses and biological activity (topoisomerases inhibition, antitumoral and antimicrobial properties) of rebeccamycin analogs bearing modified sugar moieties and substituted on the imide nitrogen with a methyl group. *J. Med. Chem.* **40**, 3456-3465.

Because *Chemistry & Biology* operates a 'Continuous Publication System' for Research Papers, this paper has been published via the internet before being printed. The paper can be accessed from http://biomednet.com/cbiology/cmb – for further information, see the explanation on the contents pages.